ОБЪЕДИНЕННЫЙ
ИНСТИТУТ
ЯДЕРНЫХ
ИССЛЕДОВАНИЙ

Дубна

E13-96-149

V.L.Aksenov, Yu.V.Nikitenko

TIME COLLIMATION FOR ELASTIC NEUTRON SCATTERING INSTRUMENT AT A PULSED SOURCE

Submitted to «Neutron Research»

1996

INTRODUCTION

The main objective of the experiment at an elastic neutron scattering spectrometer (neutron diffractometer, small-angle neutron scattering setup, neutron reflectometer) is to measure the neutron scattering cross-section(the scattering law F(q))in relation to the absolute value of the scattering vector q. The generalized scheme of the spectrometer (see Fig.1) includes angle collimation of the neutron beam in the source-sample flight path and detection of neutrons scattered by the sample at an angle θ. In the case of a spectrometer at a pulsed neutron source, the time-of-flight method is employed, making it possible to use a wide range of neutron wavelengths. As a result of a narrow spectrum width, neutrons with different wavelengths are used unequally. In the present paper, time-of-flight collimation of the phase volume of neutrons incident on the sample V_{phase} is proposed. The collimation is performed by varying the cross-section of the diafragms placed in the source-sample flight path with time t. As a result, the solid angle $\Omega(t \propto \lambda)$ at which the neutron source is visible, and the cross-section of the neutron beam on the sample $S_{beam}(t \propto \lambda)$, are chosen for each concrete neutron wavelength λ. This allows us to obtain optimal measuring conditions following certain collimation laws, when the maximum scattered neutron intensity $J_{scatt.}$ is achieved at a fixed distortion of the scattering law Res(F). In what follows, the optimization criteria are considered using the small-angle neutron scattering spectrometer as an example and then their application is demonstrated for small-angle diffusion and diffraction scattering and reflection of the neutrons.

OPTIMIZATION CRITERIA

We shall consider the optimization criteria in more detail for a small-angle scattering spectrometer. Figure 2 presents the scheme of a small-angle scattering spectrometer with axial geometry. The main functional elements of the spectrometer are: the first and the second diaphragms used for angle collimation of the incident beam, placed at distances of L_0 and $L_0+ L_1$, respectively, from the source; sample position (coincident with the second diaphragm); and, a scattered neutron detector placed at a distance $L_0+L_1+L_2$ from the neutron source. The dependence of the scattering cross-section $d\sigma(q)/d\Omega$ (the scattering law is F(q)) on the absolute value of the scattering vector $q = 4\pi\sin(\theta/2)$, where λ is the neutron wavelength and θ is the scattering angle, is measured with the spectrometer. For the intensity of the scattered beam, $J(\lambda,q)$, and the root-mean-square deviation, $\sigma_q(\lambda)$, the following relationships apply [1]:

$$J(\lambda,q) = j_0(\lambda)\, R_1^2R_2^2F(q)R\Delta R/L_1^2/L_2^2,$$

$$\sigma_q(\lambda) = \pi/\lambda((R_1/L_1)^2+R_2^2(1/L_1+1/L_2)^2+(\Delta R/L_2)^2/3+(R/L_2)^2(\Delta\lambda/\lambda)^2/3)^{1/2}, \quad (1)$$

where $j_0(\lambda)$ is the neutron flux before the first diaphragm, R_1 and R_2 are the radii of the first and second diaphragms, respectively, R and ΔR are the radius and width of the detecting element in the detector and $\Delta\lambda$ is the wavelength uncertainty.

The well-known approach in optimization [1,2] involves the achievement of maximum intensity at fixed values for the root-mean-square deviation of q, q itself, neutron wavelength and total flight path, $L_1+ L_2$. This can be attained if the following relationships are satisfied [2]:

$$L_1 = L_2\,,\ R_1 = 2R_2 = (2/3)^{1/2}\Delta R = (2/3)^{1/2}R\Delta\lambda/\lambda. \quad (2)$$

However, conditions should be schosen appropriate for the whole interval of q values. It is apparent that the scattering intensity should be represented in relation to the q [3]:

$$J = \int j_0(q)\, \Phi(q)\, dq, \quad (3)$$

where $j_0(q)$ is the scattering intensity at a definite value of q and unit value of scattering law, $\Phi(q)=\int F(q')R(q,q')dq'$ is the scattering law distorted by the resolution of q; R(q,q') is the resolution function. For $j_0(q)$ and R(q,q') the following relationships should be satisfied:

$$j_0(q) = q\int j_s(\lambda)d\lambda \quad \text{and} \quad R(q,q') = \int R(q,q',\lambda)\, j_s(\lambda)\, d\lambda \,/\, \int j_s(\lambda)d\lambda, \quad (4)$$

where $j_s(\lambda) = \lambda^2R_1^2R_2^2j_0(\lambda)$, $R(q,q',\lambda)$ is the resolution function at a definite value of λ, $\lambda_{max}=2R_{max}/qL_2$, $\lambda_{min}=2R_{min}/qL_2$ are the integration limits, R_{max} and R_{min} are the maximal and minimal radii of the detecting area of the detector.

We introduce a deviation of the scattering law $\delta F(q) = |(\Phi(q) - F(q))|$ and a root-mean-square deviation of the scattering law $\delta F_{st}(q)$, caused by the statistics of counting scattered neutrons. Now we can write the optimization conditions as follows:

$$A = \int (\delta F(q)/F(q))dq \,/\, \int dq = \text{const}$$

$$B = \int (\delta F_{st}(q)/\delta F(q))^2dq = \int (F(q)/\delta F(q))^2/(j_0(q)F(q))dq = \min. \quad (5)$$

Additional conditions are the fixed neutron spectrum and fixed wavelength interval, as well as measuring time, total neutron flight path and detector size. The relationship between the flight paths, $a=L_1/L_2$, and the relationship between the radii of the diaphragms in relation to time, starting from the moment of the pulse is initiated, $b(t)=R_1(t)/R_2(t)$, should be determined. Since the time of flight of the neutron from the source to the diaphragm is directly proportional to the neutron wavelength, b(t) can be transformed to $b(\lambda)$.

DIFFUSION SMALL-ANGLE SCATTERING

The resolution function within a certain approximation may be represented by a Gaussian [3] with a variance of the scattering vector, $D_q(q)$:

$$D_q(q) = \int \sigma_q^{-1}(\lambda)j_s(\lambda)d\lambda \,/\, \int \sigma_q^{-3}(\lambda)j_s(\lambda)d\lambda. \quad (6)$$

In this case, in the first approximation for the distortion of the scattering law, we obtain $\delta F(q) = 1/2(dF^2(q)/dq^2)D_q(q)$. Then we choose the approximations $\Delta R = 0$ and $\Delta\lambda = 0$, at which $\sigma_q(\lambda)$ is inversely proportional to the neutron wavelength and it is possible, under certain conditions, to obtain an analytical solution. This takes place in practice and is realised for the case of high luminosity, when the resolution is determined only by the sizes of the neutron source and the sample. Let us next represent the diaphragm radii as $R_1 = R_{10}(\lambda/\lambda_{min})^n$ and $R_2 = R_{20}(\lambda/\lambda_{min})^n$. The problem can be formulated as follows: optimal values of the a,b and n parameters should be determined so that conditions (5) are fulfilled. To this end the equation $dB/dX = 0$, where X = a,b,n, should be satisfied. This gives us a=1 and b=2.

To determine the optimal value of the n parameter, numerical calculations should be made. Figure 3 presents the results of these calculations. When carrying out the calculations, the Maxwellian spectrum with a characteristic wavelength λ_t = 1.8 Å was taken. The following parameter values were chosen: $L_1 = L_2 = 40$m, R_{min} = 5cm and R_{max} = 50cm. The wavelength interval 0.5 - 10Å corresponds to the q interval 0.0008 - 0.16Å^{-1}. The dependence of parameter $\eta(n) = B(n=0)/B(n)$ (hereinafter referred to as the gain factor) for different scattering laws is given in Fig.3. From this figure we notice that for the 1/q law (curve 1) the maximum for $\eta(n)$ is achieved at n = -0.98. For the $\exp(-pq^2)$ law the maximum for $\eta(n)$ is at

positive values of the n parameter (curves 2 and 3). As an illustration, Fig.4 shows the dependence $\delta F_{st}^2(q)/\delta F^2(q)$ for the scattering law $F(q) = \exp(-100(\text{Å}^2)q^2)$ for n=0 and n=1/4. It is seen from the figure that in certain regions, where q varies, curve 1 goes below curve 2. One can see, however, that curve 2 (n=1/4) runs integrally below curve 1 (n=0). This means that the mode with n=1/4 is more optimal. We also notice that at large q, the statisticaling accuracy decreases.

NEUTRON REFLECTION

Figure 5 presents the scheme of the reflectometer. The neutron beam is incident on the sample at a grazing angle θ . Two diaphragms, placed in the XZ plane at distances L_1 and L_2 from the source, are used to collimate the beam. Assume that the diaphragm sizes are considerably greater in the X-axis direction than in the Z-axis direction. Then, for the variance of the wave vector transfer, p, we have ($\Delta\lambda$ is assumed to be 0):

$$D_p(p) = k^2 \cos^2(\theta)(z_1^2 + z_2^2)/3L_0^2, \qquad (7)$$

where k is the wave vector, z_1 and z_2 are the diaphragm sizes in the direction of the Z-axis, $L_0 = L_2 - L_1$, $p=2k\sin(\theta)$

The following relation holds for $j_0(p)$:

$$j_0(p) = j_0(\lambda)z_1(\lambda)x_1z_2(\lambda)x_2/ L_0^2/p^2 \quad , \qquad (8)$$

where x_1 and x_2 are the diaphragm sizes in the direction of the X-axis. Let us represent z_1 and z_2 as $z_1 = z_2 = z_0 (\lambda/\lambda_{min})^n$. Figure 6 gives the $\eta(n)$ dependence for different reflection laws at the angle of reflection $\theta = 6$ mrad and wavelength interval 0.7 - 10Å. It can be seen that, as in the case of the small-angle spectrometer, the optimal n value may be either positive or negative, depending on the type of reflection law.

SMALL-ANGLE DIFFRACTION

Let us consider the case of small-angle powder diffraction. In this connection we choose a diffractometer scheme identical to the scheme for small-angle diffusion scattering spectrometer(Fig.2). Depending on q, the scattering law for the Bragg diffraction, as is well-known, is a delta-function. Therefore, the employment of conditions (5) presents difficulties. Because of this, let us formulate simplified criteria:

$$C = \int \delta q(q)/q \, dq = \text{const} \quad \text{and} \quad E = \int j_0(q)\Phi(q)dq = \max . \qquad (9)$$

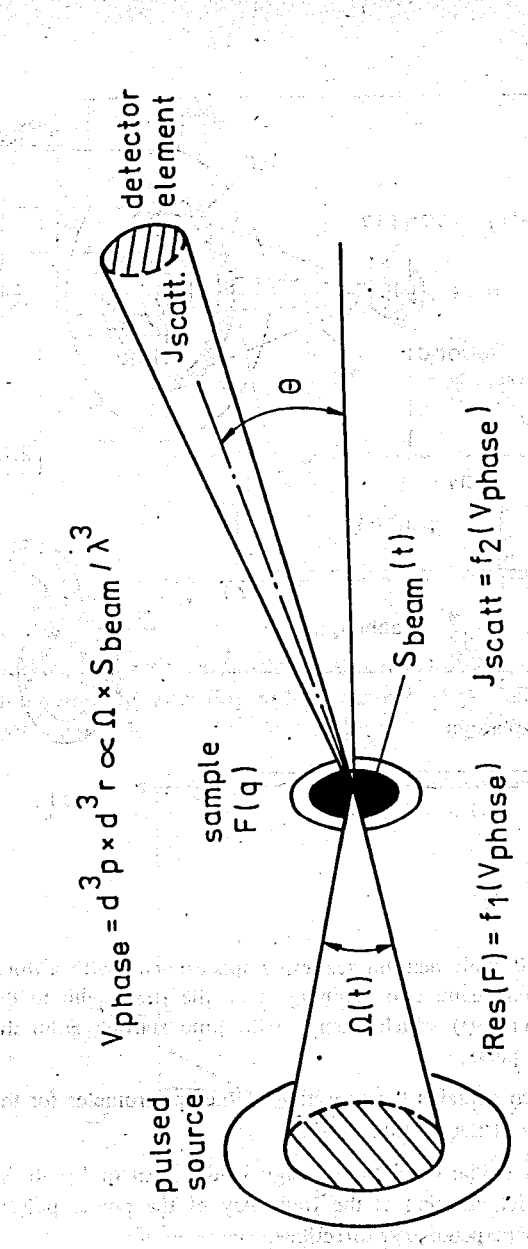

FIGURE 1 Layout of the elastic scattering neutron spectrometer with a time-of-flight collimation of the neutron beam.

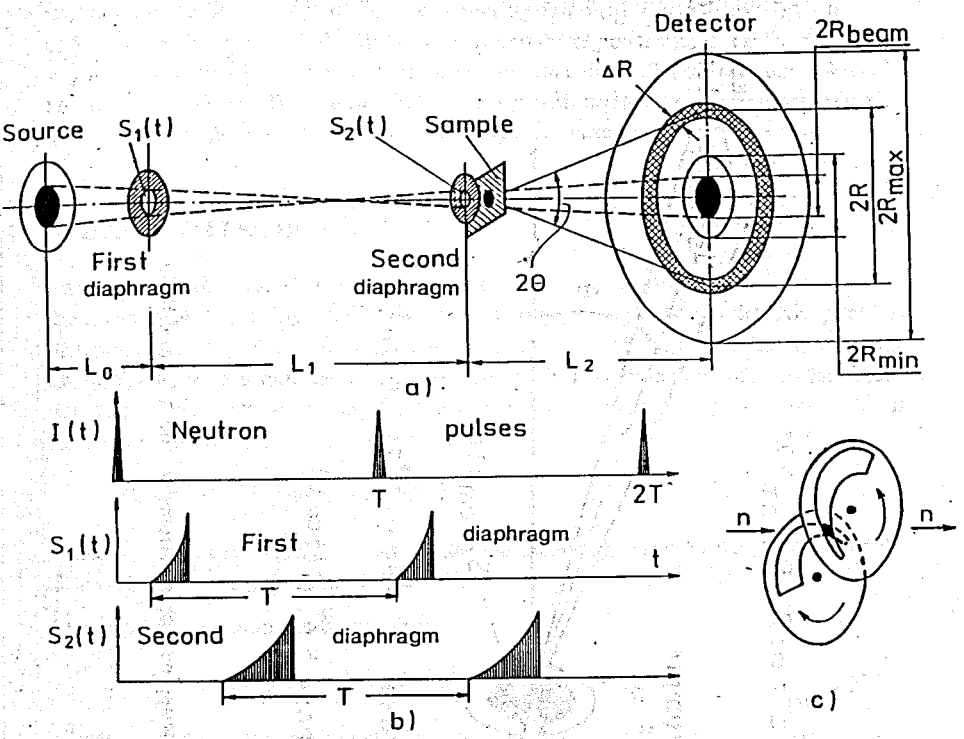

FIGURE 2 a) Scheme of the small-angle neutron scattering spectrometer with a time-of-flight collimation of the neutron beam: two diaphragms on the flight path to the sample have an area of $S_1(t)$ and $S_2(t)$ which change with time starting from the moment of initiation of the source pulse;

b) time diagram which explains the operation of the spectrometer for the period T of recurring power pulses of the neutron source;

c) a possible version of the diaphragm design in the form of two disks made of absorbing neutron material, rotating at the frequency of the power pulses. Slots in the disks meet in mutually perpendicular directions.

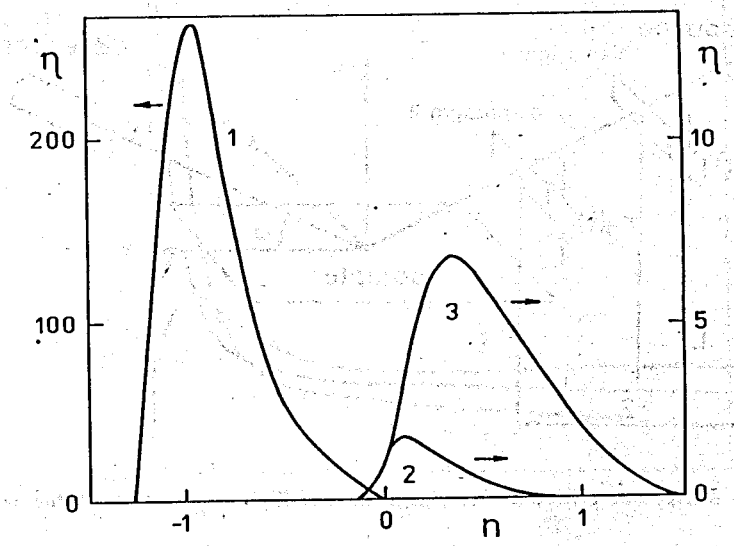

FIGURE 3 Dependence of the $\eta(n)$ parameter for different small-angle diffusion neutron scattering laws: $F(q) = 1/q$ - curve 1; $F(q) = \exp(-pq^2)$ and $p=10Å^2$ - curve 2, $p=100Å^2$- curve 3.

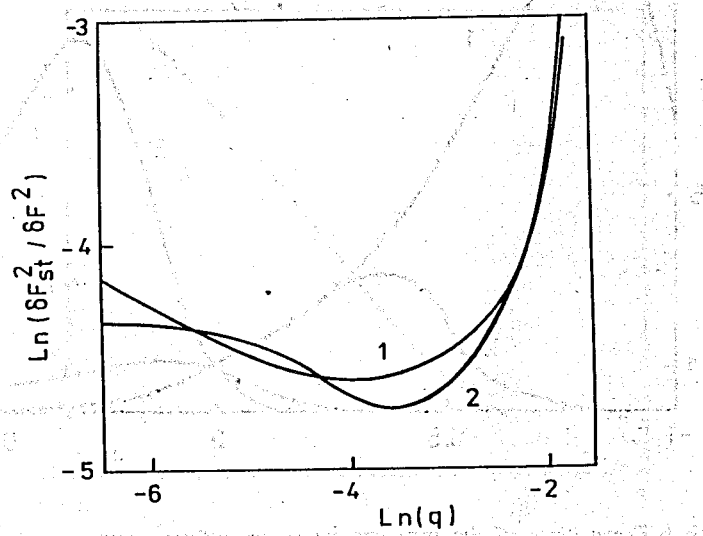

FIGURE 4 Dependence of $\delta F^2_{st}(q)/\delta F^2(q)$ for the scattering law $F(q) = \exp(-100q^2)$ at different values for the n parameter: 1- n=0; 2 - n=1/4.

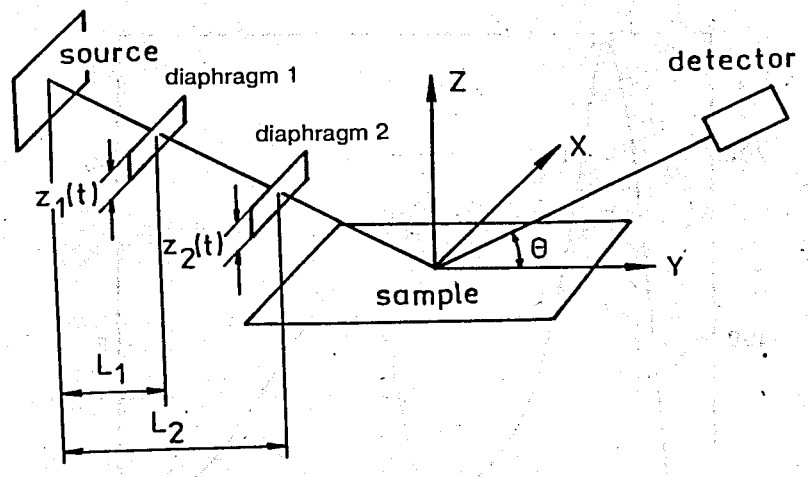

FIGURE 5 Neutron reflectometer with a time-of-flight collimation of the neutron beam.

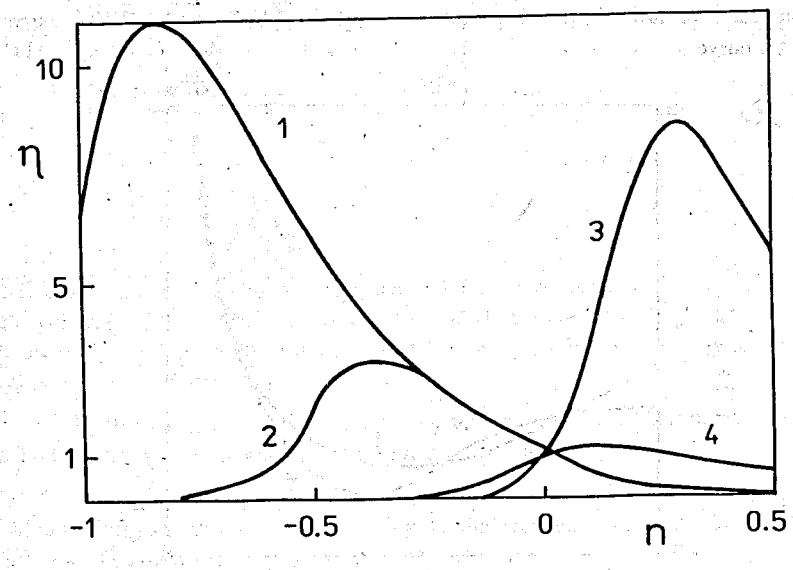

FIGURE 6 Dependence of the η(n) parameter for different neutron reflection laws: $F(q) = q^{-4}$ - curve 1; $F(q) = q^{-1}$ - curve 2; $F(q) = \exp(-rq)$ and r = 50 Å - curve 3, r = 100 Å - curve 4.

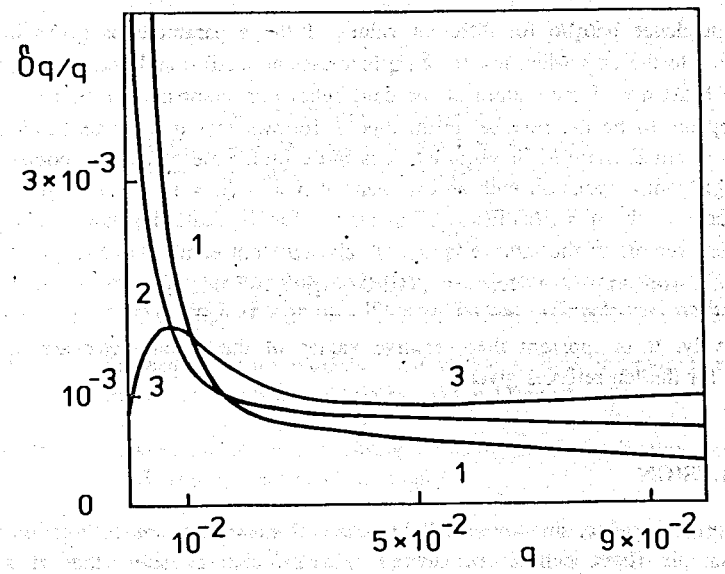

FIGURE 7 Dependence of δq(q)/q at different values of the n parameter: 1- n=1, 2 - n=0, 3 - n=-1.

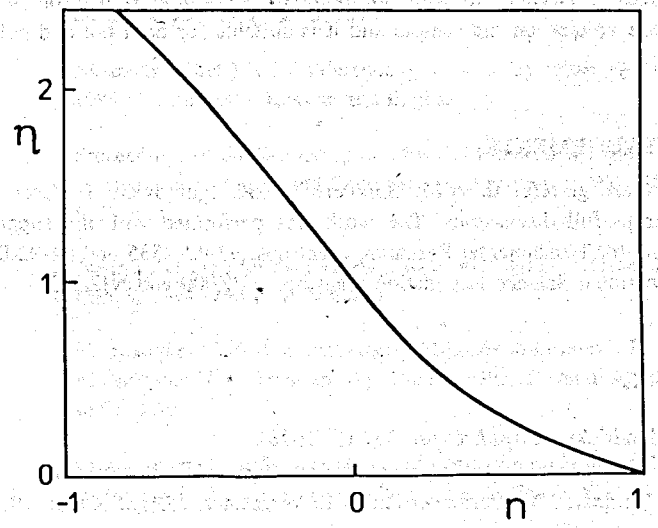

FIGURE 8 Dependence of the η=E(n)/E(n=0) parameter for the case of ten reflexes in the Bragg neutron diffraction.

The dependence $\delta q(q)/q$ for different values of the n parameter is given in Fig.7. Compared to the case when n = 0, $\delta q/q$ increases at small q and decreases at large q for n = 1. At n = -1 the pattern of the $\delta q/q$ behaviour, compared to the case when n = 0, appears to be the reverse. From this, it follows that if a higher resolution of reflexes at small (large) q is required, it is more preferable to use the power law of diaphragm radius variation with an exponent of n = -1 (n = 1). Figure 8 presents the dependence of the $\eta = E(n)/E(n = 0)$ parameter for the scattering law $F(q) = \sum_\tau \delta(q-q_\tau)$, where vectors of the inverse lattice are chosen from condition $(q_j-q_{j-1}) \sim (q_j+q_{j-1})$ and equal (in units $Å^{-1}$) to: q_1=7.94E-04, q_2=8.16E-04, q_3=8.7E-4, q_4=1.0E-03, q_5=1.35E-03, q_6=2.2E-03, q_7=4.345E-03, q_8=9.7E-03, q_9=2.31E-02, q_{10} =5.65E-02 respectively. It is apparent that negative values of the n parameter are the most optimal for the ten reflexes given.

CONCLUSION

In the present paper, the time-of-flight mode of neutron beam collimation in the source-sample flight path is considered. The calculations show that at a fixed distortion of the scattering law and following certain collimation laws, the statistical accuracy of measurements increases greatly. The proposed operating regime for the elastic scattering spectrometers is simple to realise. Its use is the most effective at low-frequency pulsed sources where a broad wavelength interval is available. This method makes it possible to form an optimal (according to neutron wavelength) neutron phase volume on the sample and it is suitable for both hot and cold neutron sources.

ACKNOWLEDGEMENTS

The authors are grateful to A.M. Balagurov, V.K. Ignatovich, L. Cser and B.N. Savenko for usefull discussions. The work was performed with the support of the Russian Fund for Fundamental Research, grant nos. 93-02-2535 and 94-02-04011 and of the International Science Foundation grant nos. NJZ000 and NJZ300.

REFERENCES

[1] R.W. Hendricks, *J. Appl. Cryst.* **11**, 15 (1978).

[2] D.F.R. Mildner and J.M. Carpenter, *J. Appl. Cryst.* **17**, 249 (1984).

[3] D.F.R. Mildner, J.M. Carpenter and D.L. Worcester, *J. Appl. Cryst.* **19**, 311 (1986).

Received by Publishing Department
on April 25, 1996.